www.sciencemag.org/cgi/content/full/339/6126/1445/DC1

Supplementary Materials for

A Localized Wnt Signal Orients Asymmetric Stem Cell Division in Vitro

Shukry J. Habib,* Bi-Chang Chen, Feng-Chiao Tsai, Konstantinos Anastassiadis, Tobias Meyer, Eric Betzig, Roel Nusse*

*Corresponding author. E-mail: rnusse@stanford.edu (R.N.); shabib@stanford.edu (S.J.H.)

Published 22 March 2013, *Science* **339**, 1445 (2013)
DOI: 10.1126/science.1231077

This PDF file includes:

Other Supplementary Material for this manuscript includes the following:
(available at www.sciencemag.org/cgi/content/full/339/6126/1445/DC1)

Materials and Methods

Production and immobilization of Wnt proteins

Recombinant mouse Wnt3a or Wnt5a proteins were produced in Drosophila S2 cells grown in suspension culture, and purified by Blue Sepharose affinity and gel filtration chromatography as described (30). Wnt3a activity was determined in a luciferase reporter assay using L cells stably transfected with the SuperTOPFlash reporter as described (10)/ (fig. S2). Wnt3a or Wnt5a were immobilized onto 2.8 μm Dynabeads® M-270 Carboxylic Acid (Invitrogen). The carboxylic acid groups were activated at room temperature for 30 min by carbodiimide and N-hydroxyl succinimide (50mg/ml each, dissolved in 25mM cold 2-(N-morpholino)ethanesulfonic acid (MES) buffer pH 5). After activation the beads were washed three times with 25mM MES buffer pH 5. To achieve Wnt immobilization, 0.2 μg of purified Wnt protein was diluted 1:5 in cold MES pH 5 and incubated at room temperature with gentle rocking for one hour. The Wnt beads were washed three times with MES pH 5 and additional three times with phosphate buffered saline (PBS) pH 7.4. The Wnt beads were stored in PBS/ 1% BSA buffer at 4°C. To generate inactive variants of immobilized Wnt3a, Wnt3a protein was immobilized onto beads followed by incubation with Dithiothreitol (DTT) for 12 min at 37°C. Then, the Wnt beads were washed six times with PBS and stored in PBS/ 1% BSA buffer at 4°C. Wnt5a activity was determined by inhibiting Wnt3a activity in a luciferase reporter assay using 293 cells stably transfected with the SuperTOPFlash reporter as described (2). Purified R-spondin-1 and DKK-1 proteins were purchased from R&D systems. 6 μg purified R-spondin-1 were covalently immobilized onto 2.8 μm Dynabeads® M-270 Carboxylic Acid (Invitrogen) as described above. To immobilize DKK-1, 10 μg aldehyde coated beads (5 micron, Xenopore) were washed three times with PBS and then incubated with 4 μg purified DKK1 for one hour. The DKK-1 beads were washed with PBS three times and stored in PBS/ 1% BSA buffer at 4°C.

Cell lines and Cell culture

Mouse Embryonic Stem (ES) cells were cultured in ES cell medium (DMEM plus 15% fetal bovine serum (Hyclone), 1mM sodium pyruvate, MEM non-essential amino acids, 50 mM b-mercaptoethanol, 100 U ml^{-1} penicillin, 100 mg ml^{-1} streptomycin (all from Invitrogen) and 1,000 U ml^{-1} LIF (Chemicon)) supplemented with 100 ng ml^{-1} Wnt3a protein on gelatin-coated plates. After the second passage, ES cells were cultured over night and then switched to N2B27 medium (6) consisting of one volume of DMEM/F12 combined with one volume of Neurobasal medium supplemented with 0.5% N2 Supplement, 1% B27 Supplement, 0.033% BSA 7.5% solution, 50 mM b-mercaptoethanol, 2mM Glutamax, 100 U ml^{-1} penicillin and 100 mg ml^{-1} streptomycin (all from Invitrogen) with 100 ng ml^{-1} Wnt3a protein. Media and recombinant proteins were changed daily in all experiments except where indicated otherwise.

After 3-5 days, the cells formed colonies and were ready to be passaged. For time-lapse imaging of single cells, the colonies were washed twice with DPBS and then incubated with cell dissociation buffer (Gibco) at 37 °C for 5 minutes followed by gentle re-suspension until a single cell suspension was achieved as determined by light microscopy. The cells were pelleted and resuspended in N2B27 medium or N2B27 medium supplemented with MEK inhibitor PD0325901 (1 μM) and GSK3 inhibtor CH99021 (3μM) together known as 2i (8). ES Cell lines: Sox2-GFP ES cells (21), a gift from Dr. Konrad Hochedlinger; Stella-GFP ES cells (31), a gift from Dr. Azim Surani; OCRG9 ES cells (19), a gift from Dr. Hitoshi Niwa; H2B-Venus ES cells (32), a gift from Dr. Timm Schroeder; female LF2 ES cells (33), a gift from Dr. Joanna Wysocka, Stanford.

The Nanog-Venus and Oct4-Venus knock-in lines were generated by gene targeting in R1 ES cells. A Venus-IRES-neo cassette was inserted before the stop codon and in frame with the coding sequence of the gene.

Plasmids and mESC transfection

pEGFP-CENT1 (14) was obtained from Dr. Song Hai Shi. The mouse ninein (GenBank/EMBL/DDBJ accession number AY515727) plasmid was provided by Dr.

Michel Bornens. XE241 Rat frizzled-1-GFP-CS2P+ was purchased from Addgene (Plasmid 16817).
Transient transfections were performed with X-tremeGene HP-DNA transfection reagent on mESCs according to the manufacturers instructions (Roche). At 24 h post-transfection, cells were plated onto a 6 well plate, allowed to recover for 6-8 hours and then prepared for time-lapse imaging experiments.

Marker staining and immunohistochemistry

For immunostaining, chambered coverglasses were coated with 15 mg ml^{-1} human plasma fibronectin (Sigma). 5000 cells/well were cultured with 2.25 μg Wnt beads in N2B27 medium. After 16 hours the cells were washed with DPBS and fixed with 4% paraformaldehyde for 30 min at 4°C, washed thrice with Staining buffer (0.1% BSA, 0.001% Tween 20, and 0.05% sodium azide in PBS), and blocked with 10% normal donkey serum (NDS)/Staining buffer for 30 min. Samples were then incubated with 1:200 primary antibody in Staining buffer overnight at 4°C, washed three times with Staining buffer and detected with 1:600 dilution of secondary antibodies (Alexa fluor 594, Alexa fluor 647) followed by confocal imaging. The primary antibodies used were: APC (Santa Cruz, sc 7930), anti-H3K27me3 (active motif 39158), anti Ninein (abcam, ab4447), anti-Claudin6 (Santa Cruz, sc17669), anti-Stella (abcam, ab19878), anti-Rex1 (abcam, ab28141), anti ß-catenin (BD 610154) and anti-Lrp6(T1479) a gift from Dr. Gary Davidson.

Confocal imaging

The Zeiss Meta LSM510 confocal was utilized and a series of Z stack images were collected with either 63x/NA 1.4 oil or 40x/NA 1.3 oil objective. The Z series were analyzed by Volocity software (PerkinElmer). Only a fine filter was applied to reduce the noise in the image. A three dimensional reconstruction was performed and a snapshot was made and represented in JPEG image format. Some of the panels contain XYZ views.

Two-dimensional time-lapse imaging

Cell preparation: Single cell suspension of 5000 reporter ES cells (in N2B27 media) were mixed with 2.25 µg Wnt beads and co-cultured in 8 well chambered coverglass slides. The cells and beads were incubated for 1 h at 37°C and 5% CO2 before starting the time-lapse experiment.

Time-lapse microscopy for all experiments was performed using a DMI6000 B system (Leica) at 37°C and 5% CO2. Bright field and fluorescence images were acquired every 20 to 30 min using 20x/NA 0.7 or 40x/NA 0.75 objective, a Cascade II camera (1024x1024), a 300 W Xenon lamp and Metamorph acquisition software (Molecular Devices). Metamorph software or Image J software were used for image analysis and for the generation of movies (QuickTime and AVI). In some of the analysis, a Gaussian blur filter (2x2) was used to reduce the noise in fluorescence images and the image contrast was manually enhanced for optimal recognition of the relevant cellular features separately for each wavelength. All individual frames of time-lapse acquisition are displayed as JPEG image format. All cell tracking was done manually; the presented analysis does not rely on data generated by an unsupervised computer algorithm for automated tracking. Only single cells contacting one bead or more that could be identified clearly were used for analysis, and all cells touching other cells or with questionable identity were excluded from the analysis.

Signal intensity quantification of Nanog-Venus: for each frame, the cells were recognized using both the contrast of the bright-field image and the fluorescent signals from the Nanog-Venus image. The Nanog-Venus image was then processed by local background subtraction. The mean and standard deviation of the Nanog signal intensity from each cell are determined by all the pixels within the mask, excluding the pixels of the 50 highest and the 50 lowest intensities. Student's-t test was used to examine the difference between the cell with bead(s) and the one without bead(s). All above processes were performed using Matlab 7.11.0 (Mathwork.)

Bessel beam plane illumination microscopy

Mouse ES cells expressing H2B-Venus protein were mounted onto 18mm coverslips at a 45° angle in the y–z plane defined by the axes of excitation and detection objectives, and translated with sample stages to place the desired part of the specimen in the imaging volume. The sample chamber was filled with N2B27 media. For time-lapse movies, approximately 150-250 two-dimensional images comprising a 40μm thick three-dimensional volume were captured every 30-60 seconds with 488nm excitation. Point spread functions were calculated, and images were deconvolved as previously described (17). Three-dimensional renderings were created using Amira software (Visage Imaging) or Volocity (PerkinElmer). The voxel size of an image is 133 nm, 133nm, 150 nm in x, y, z planes respectively.

Statistics: The P-values in Fig 3B and supplementary figures 7 and 8 were calculated according to Student's-t test. The P-values for the asymmetric inheritance of centrosomes were calculated according to binomial distribution with an expected probability of 0.5. All the rest of the P-values were calculated according to Fisher exact probability test. The P-values are calculated for the same category in Wnt3a versus Wnt5a bead treatments except where indicated otherwise.

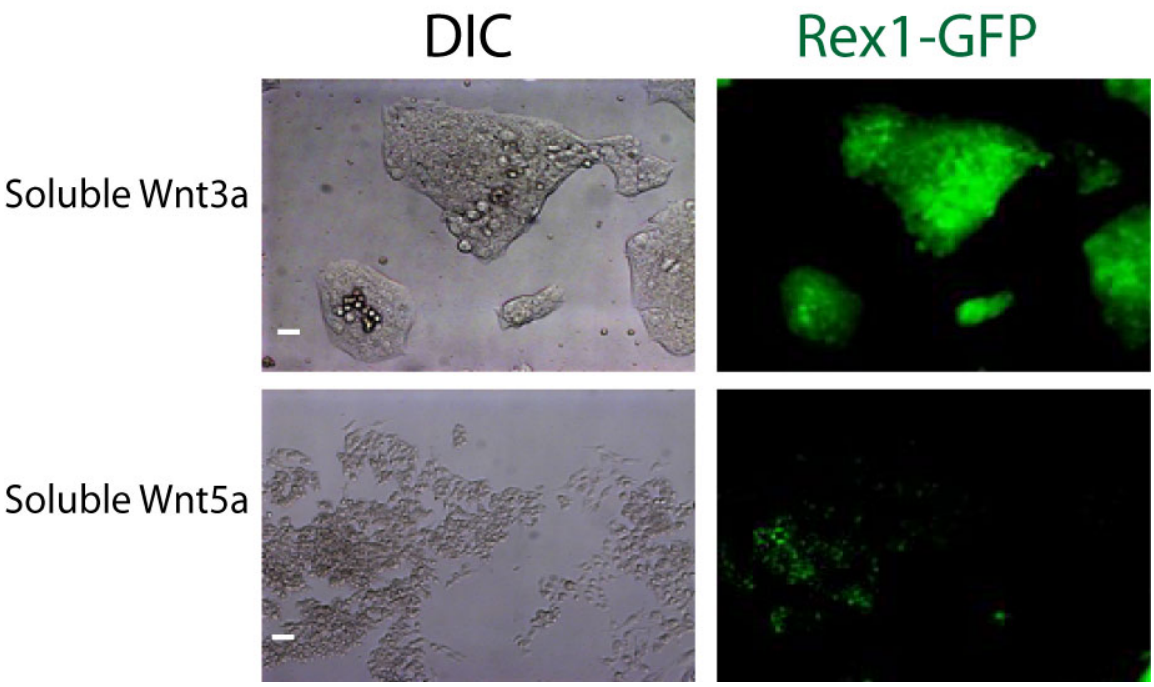

Fig. S1

Purified Wnt3a but not Wnt5a proteins support self-renewal of ES cells. Rex1-GFP ES cells were cultured for a week in serum free media in the presence of LIF and either purified Wnt3a or Wnt5a.

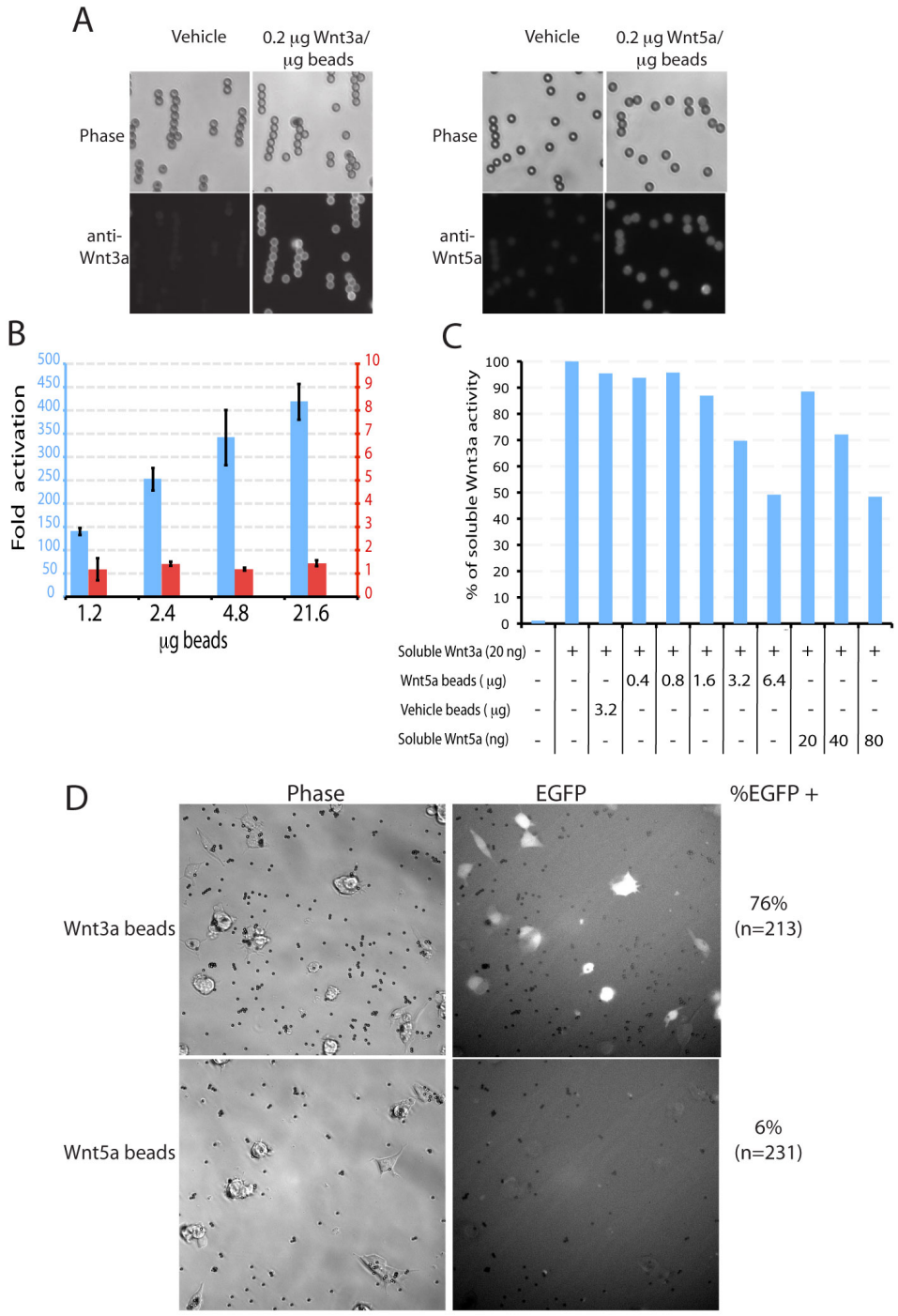

Fig. S2

Biological activity of immobilized Wnt3a and Wnt5a proteins. **(A)** Purified Wnt3a or Wnt5a proteins were immobilized onto magnetic beads and visualized by immunostaining. **(B)** Wnt3a bead (blue bars) but not vehicle bead (red bars) treatment for 24 hrs activates the SuperTopflash (STF) luciferase Wnt reporter in a dose-responsive manner. Error bars represent SD. **(C)** Wnt5a bead treatment inhibits soluble Wnt3a-induced STF reporter activation. **(D)** Wnt3a bead (black dots) treatment for 12 hrs activates the 7xTcf eGFP reporter in ES cells. The beads are 2.8 μm and can be used as a scale bar.

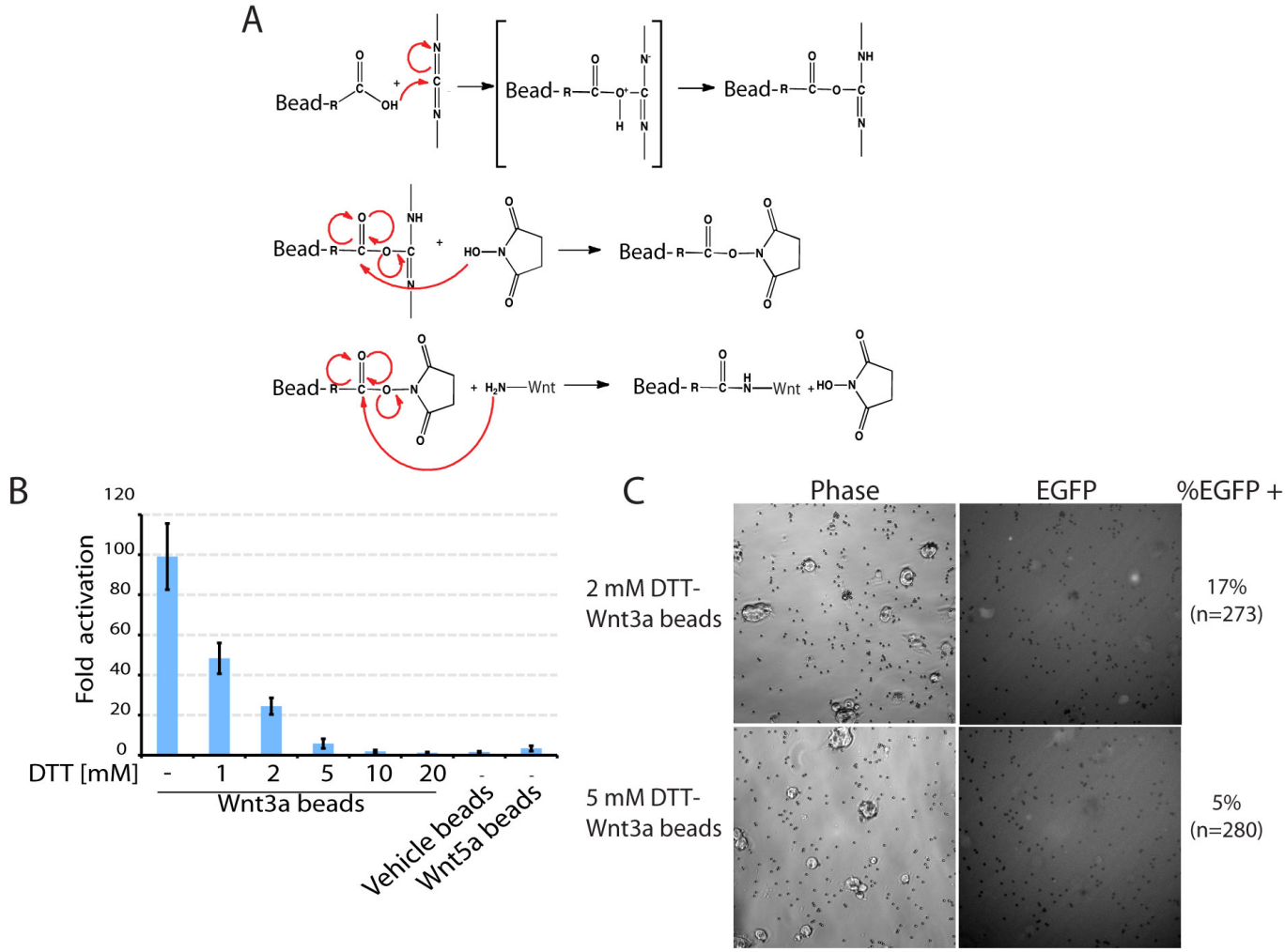

Fig. S3

Inactivation of immobilized Wnt3a proteins by DTT treatment. **(A)** The chemistry of immobilizing purified Wnt proteins onto carboxylic acid beads. **(B)** Immobilized Wnt3a proteins were treated with different concentrations of DTT and the activity of the beads was assayed for SuperTopflash (STF) luciferase Wnt reporter activity of L cells. Error bars represent SD. **(C)** DTT treated Wnt3a beads (black dots) were incubated with 7xTcf eGFP reporter ES cells for 12 h and the number of eGFP positive cells was counted. The beads are 2.8 μm and can be used as a scale bar.

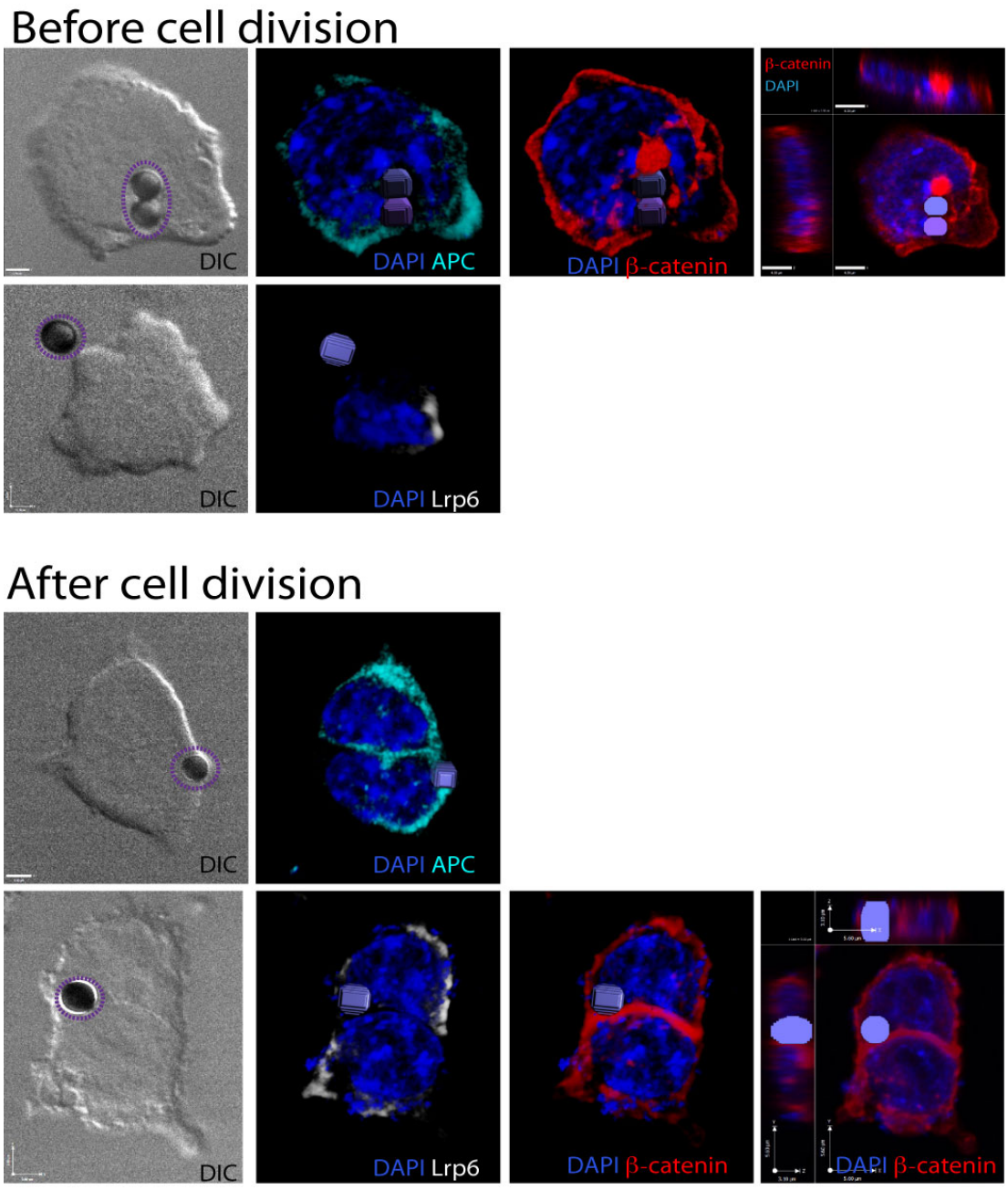

Fig. S4

Wnt5a beads do not induce asymmetric distribution of components of the Wnt/ß-catenin pathway. ES cells were co-cultured with Wnt5a beads (indicated by dashed purple circle or reconstructed as a purple oval) and immuno-stained at various stages of cell division with APC (cyan), LRP6 (white) and ß-catenin (red) antibodies. All fluorescent images are snapshots of 3D reconstruction of z stacks of the confocal images. Nuclear ß-catenin is additionally visualized by representation in XYZ in the plane of the nucleus. The beads are 2.8 µm.

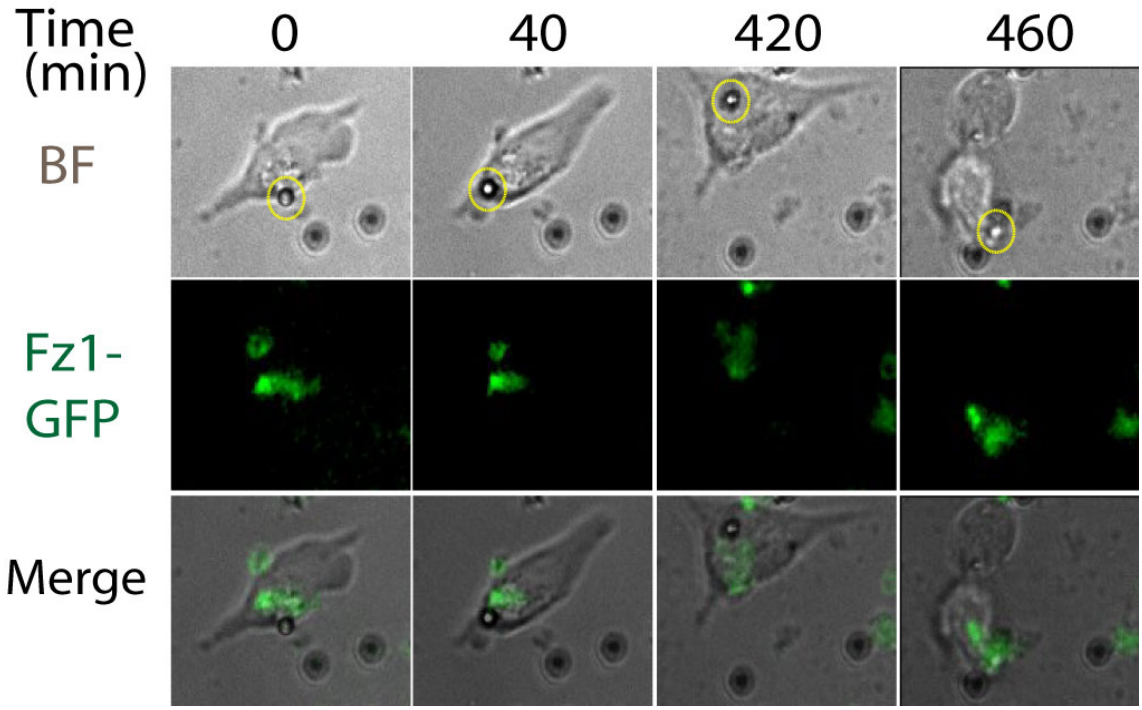

Fig. S5

The distribution of Frizzled-1(Fz1)-GFP during ES cell division. ES cells expressing Fz1-GFP were co-cultured with Wnt3a beads and the division was monitored by time-lapse imaging. The location of the bead (2.8 μm) that contacted the cell during the division is marked by dashed yellow circle.

A

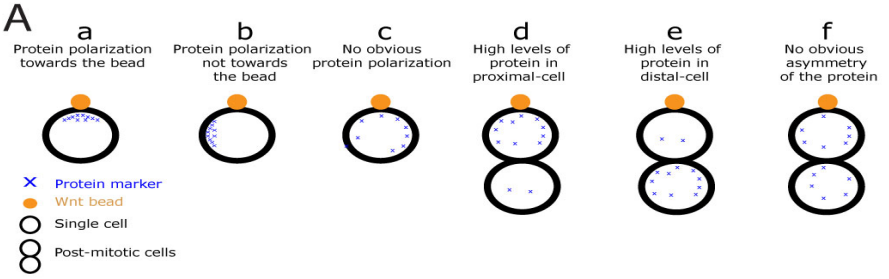

Protein	Wnt3a beads		Wnt5a beads		2mM-DTT Wnt3a beads		5mM-DTT Wnt3a beads	
	Cell #	% of total	Cell #	% of total	Cell #	% of total	Cell #	% of total
APC								
a	27	64%	11	24%	17	29%	7	15%
b	5	12%	2	5%	7	12%	5	11%
c	10	24%	32	71%	35	59%	35	74%
Total	42		45		59		47	
d	33	69%	5	12%	21	34%	4	8%
e	5	10%	3	7%	8	13%	6	12%
f	10	21%	33	81%	32	53%	41	80%
Total	48		41		61		51	
Lrp6								
a	30	65%	13	21%	23	39%	18	31%
b	5	11%	13	21%	6	10%	10	16%
c	11	24%	36	58%	30	51%	31	53%
Total	46		62		59		59	
d	30	68%	13	25%	19	32%	9	24%
e	6	14%	8	16%	5	8%	4	11%
f	8	20%	30	59%	35	60%	25	65%
Total	44		51		59		38	
β–catenin								
a	20	61%	6	20%	11	31%	4	13%
b	6	18%	3	10%	5	13%	2	6%
c	7	21%	21	70%	20	56%	25	81%
Total	33		30		36		31	
d	18	60%	3	10%	12	28%	6	18%
e	7	23%	3	10%	6	14%	4	12%
f	5	17%	23	80%	25	58%	23	70%
Total	30		29		43		33	
Rex1-GFP								
d	24	67%	4	9%	13	31%	5	14%
e	3	8%	1	3%	5	12%	4	10%
f	9	25%	40	88%	24	57%	28	76%
Total	36		45		42		37	

B

Fisher Exact Probability test- P values

	a (Wnt3a bead: Wnt5a bead)	a (Wnt3a bead: 2mM-DTT Wnt3a bead)	a (Wnt3a bead: 5mM-DTT Wnt3a bead)
APC	0.00023	0.00052	0.0000025
Lrp6	0.0000041	0.010479	0.000707
β–catenin	0.001867	0.016097	0.000093

	d (Wnt3a bead: Wnt5a bead)	d (Wnt3a bead: 2mM-DTT Wnt3a bead)	d (Wnt3a bead: 5mM-DTT Wnt3a bead)
APC	4.70E-08	0.000493	1.35E-10
Lrp6	0.00003584	0.000352	0.0000664
β–catenin	0.0000941	0.008181	0.000812
Rex1-GFP	4.42E-08	0.002876	0.000003

Fig. S6

The effect of Wnt beads on the distribution of marker proteins in ES cells. **(A)** Wnt beads were incubated with ES cells for 16 hrs. Then, cells were fixed and the distribution patterns of components of the Wnt/ß-catenin in single cells (categories a-c) and post-mitotic cells (categories d-f) were examined. For Rex1-EGFP reporter ES cells, the effect was examined by live imaging. **(B)** The P-values for the categories (a) and (d) for the different proteins among different groups were calculated.

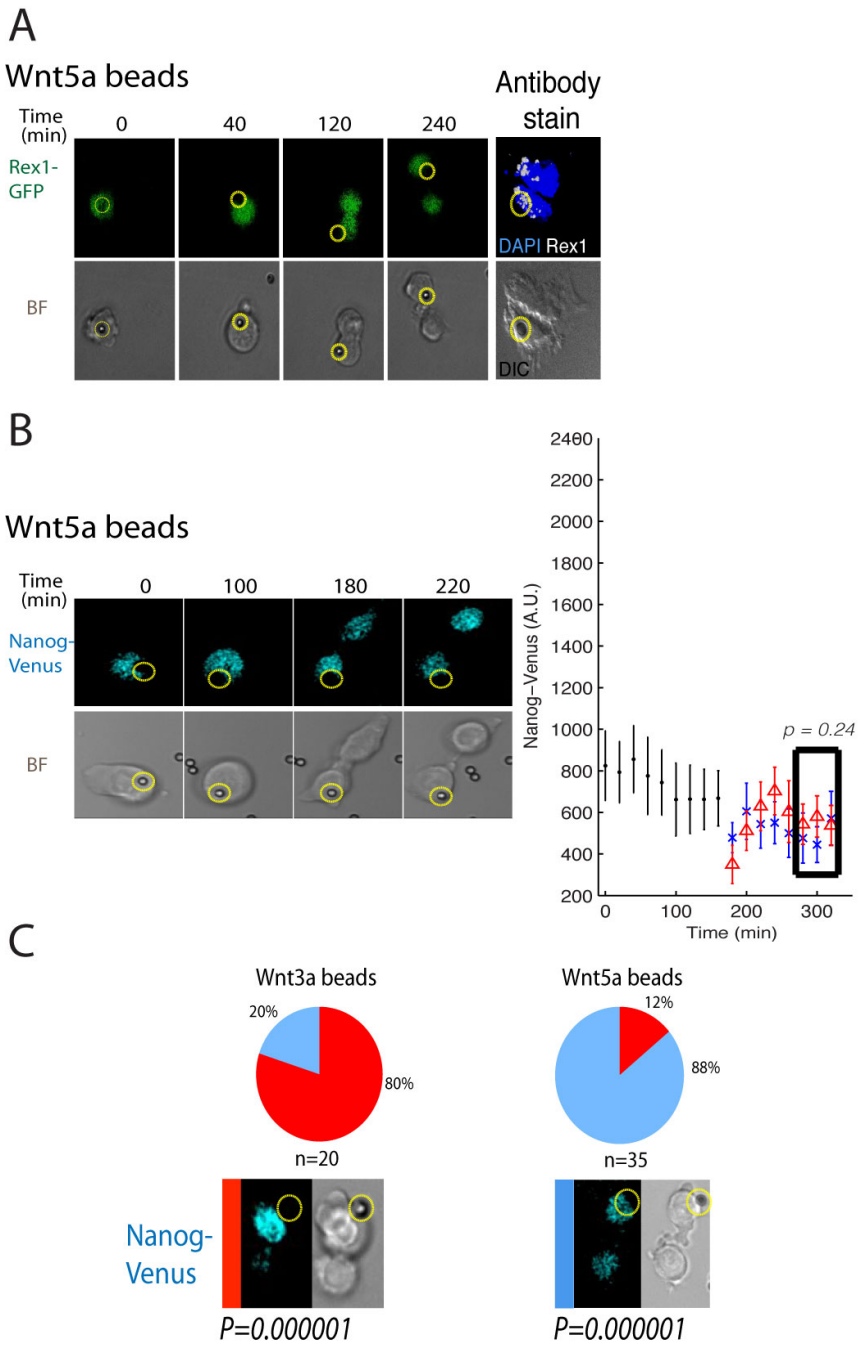

Fig. S7

Transcriptional activity of Rex1-GFP transcriptional reporter and expression of Nanog-Venus fusion protein in Wnt exposed cells. Wnt5a beads were incubated with single cells of Rex1-GFP transcriptional reporter line (**A**) or the knock in Nanog -Venus ES cell line (**B**). The protein localization during cell division was monitored by time-lapse imaging. Selected frames are shown. The brightness of the signal for each frame was determined individually. A Plot (B): The mean and SD of the Nanog-Venus signal intensity from each cell was quantified based on raw data. The signal intensity of the cell that retains contact with the bead after the division is represented with a red triangle. The blue "x" represents the distal cell. **(C)** Cell divisions were classified based on the relative expression of Nanog-Venus in the prospective daughter cells. Red bar: higher Nanog-Venus levels in the Wnt-proximal cell. Blue bar: similar levels of Nanog-Venus in both cells. The location of the bead (2.8 µm) that contacted the cell during division is marked by dashed yellow circle.

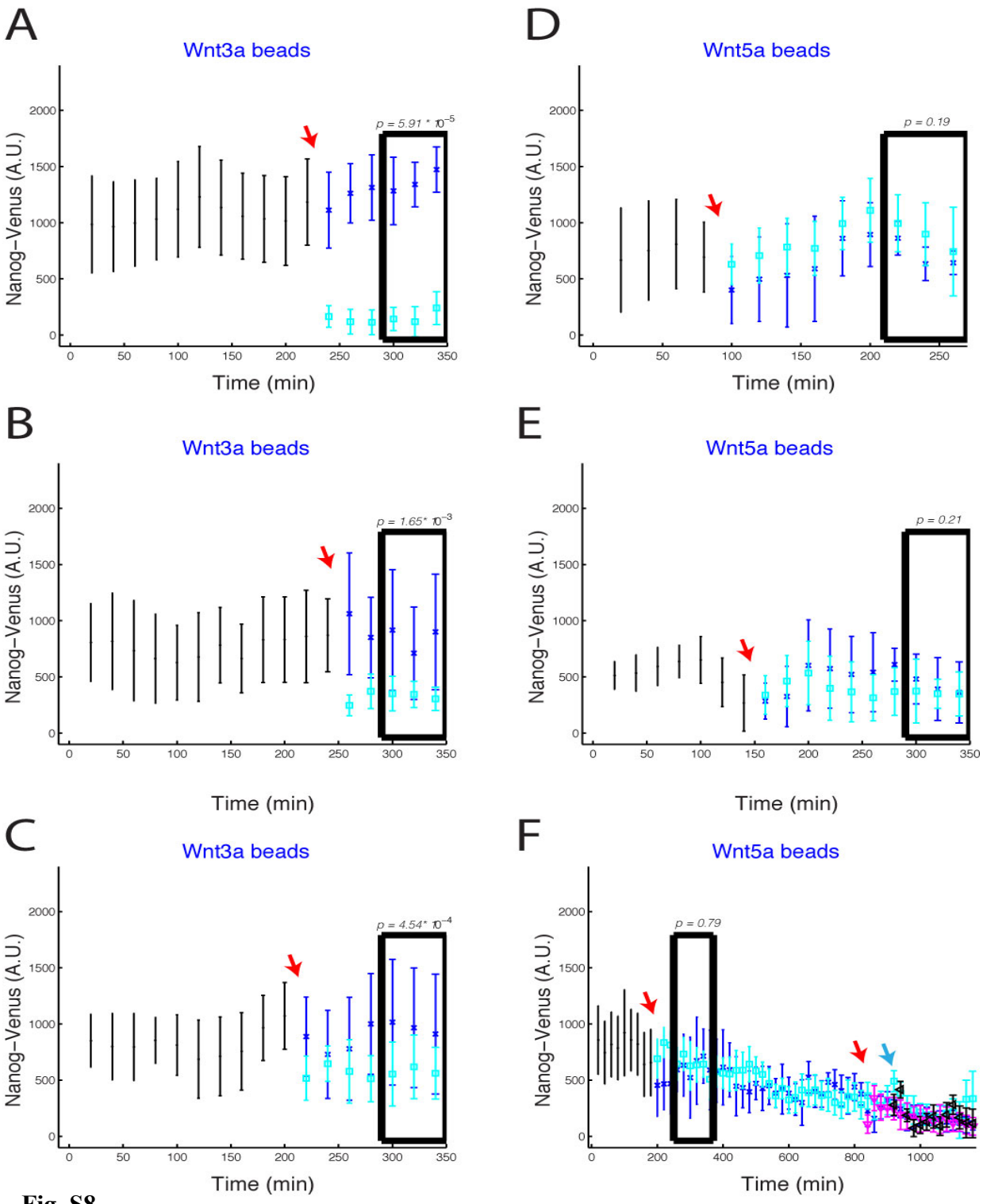

Fig. S8

Heterogeneous patterns of symmetric and asymmetric divisions in Nanog-Venus ES cells. **(A to E)** Wnt3a or Wnt5a beads were incubated with single Nanog-Venus ES cells and followed by time-lapse imaging. The mean and SD of the Nanog-Venus signal intensity in each cell was quantified based on the relative expression of Nanog-Venus in the prospective daughter cells. **(F)** Quantification of two successive divisions. (A to F) The frame of the division of the cell that contacts the bead is indicated by a red arrow. A turquoise arrow indicates the division frame of the Wnt-distal cell. The cell that contacts the bead after division is represented on the graph by blue "x".

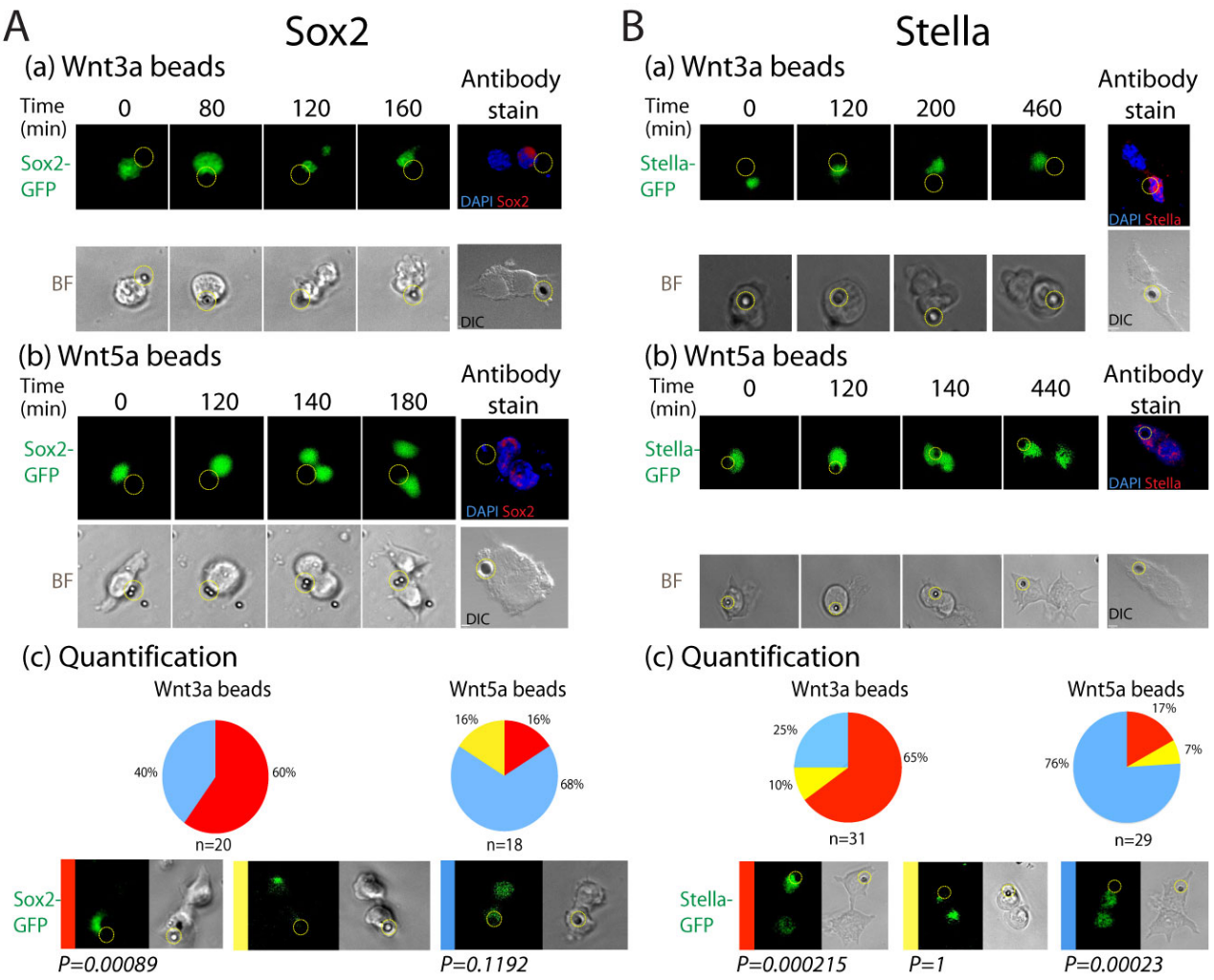

Fig. S9

Transcriptional activity of pluripotency genes during ES cell division. **(A and B)** Wnt3a (a) or Wnt5a beads (b) were co-cultured with single ES cells harboring GFP reporters under the control of promoters of Sox2 (A) and Stella (B). GFP localization was followed by time-lapse imaging. Endogenous protein localization was visualized by immunostaining of fixed cells. The cell division was quantified (c) based on the relative expression of GFP. Red bar: higher GFP levels in the Wnt-proximal cell. Yellow bar: higher levels of GFP in the Wnt-distal cell. Blue bar: similar levels of GFP in both cells. The location of the bead that contacted the cell during the division is marked by dashed yellow circle.

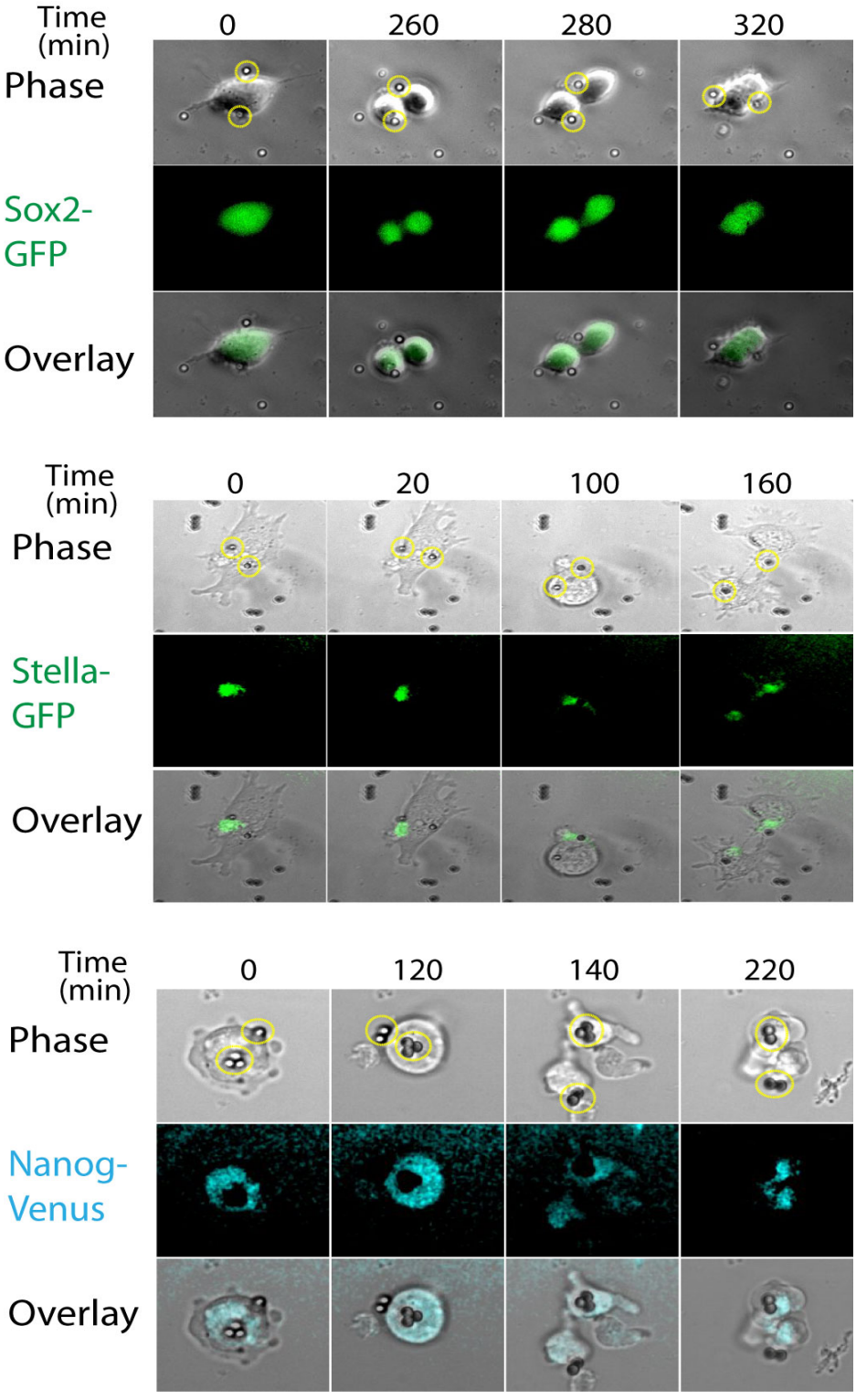

Fig. S10

ES cell division in the presence of multiple Wnt3a beads. Wnt3a beads were incubated with single cells of various pluripotency reporter lines and the division and the distribution of the beads to both daughter cells were followed by time-lapse imaging. The location of the bead (2.8 μm) that contacted the cell during the division is marked by dashed yellow circle.

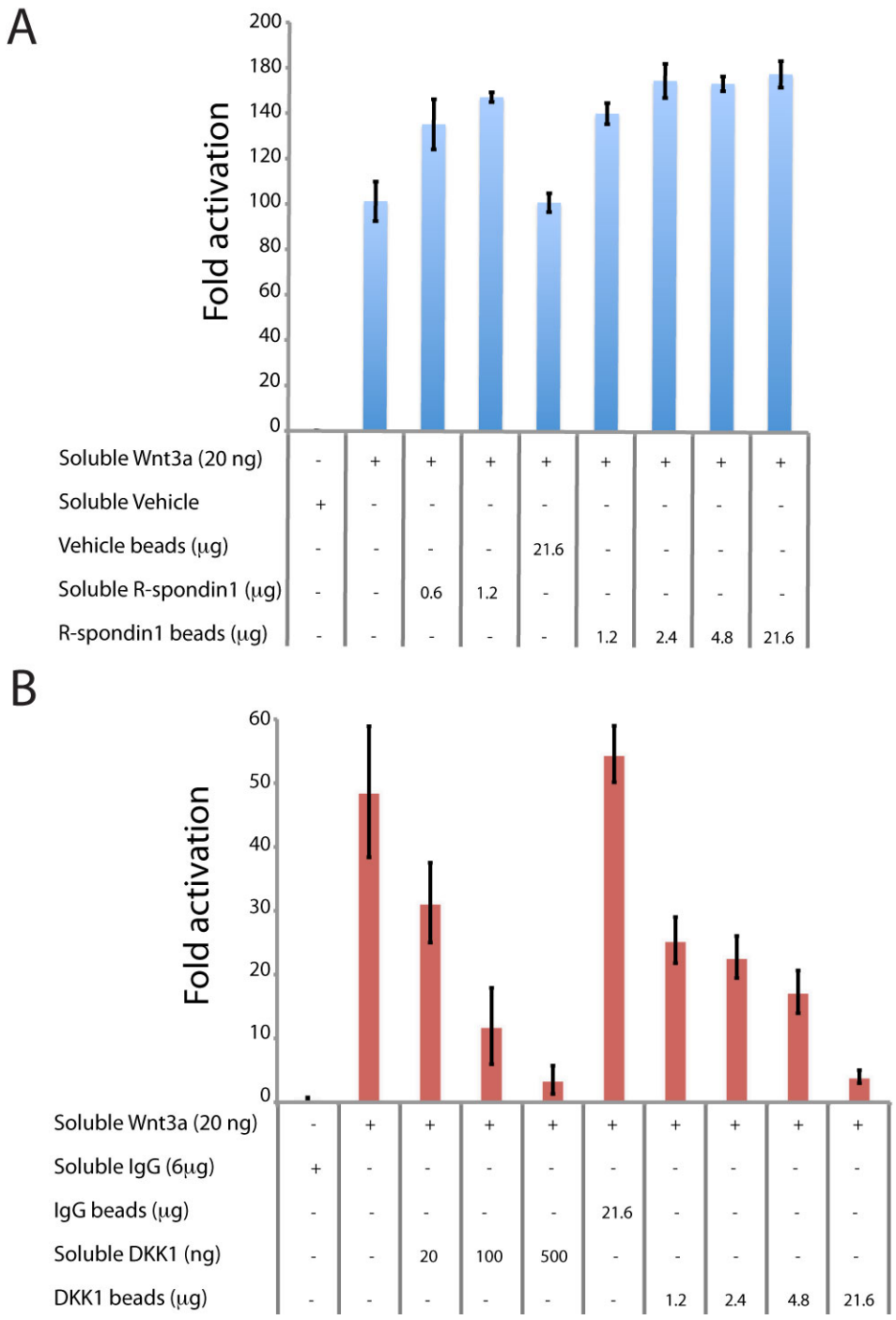

Fig. S11

Biological activity of immobilized R-spondin-1 and DKK1. **(A)** Soluble and immobilized R-spondin-1 enhance the Wnt3a-mediated activation of SuperTopflash (STF) luciferase Wnt reporter in a dose-responsive manner. **(B)** Soluble and immobilized DKK-1 inhibit the Wnt3a-mediated activation of SuperTopflash (STF) luciferase Wnt reporter in a dose-responsive manner. Error bars represent SD.

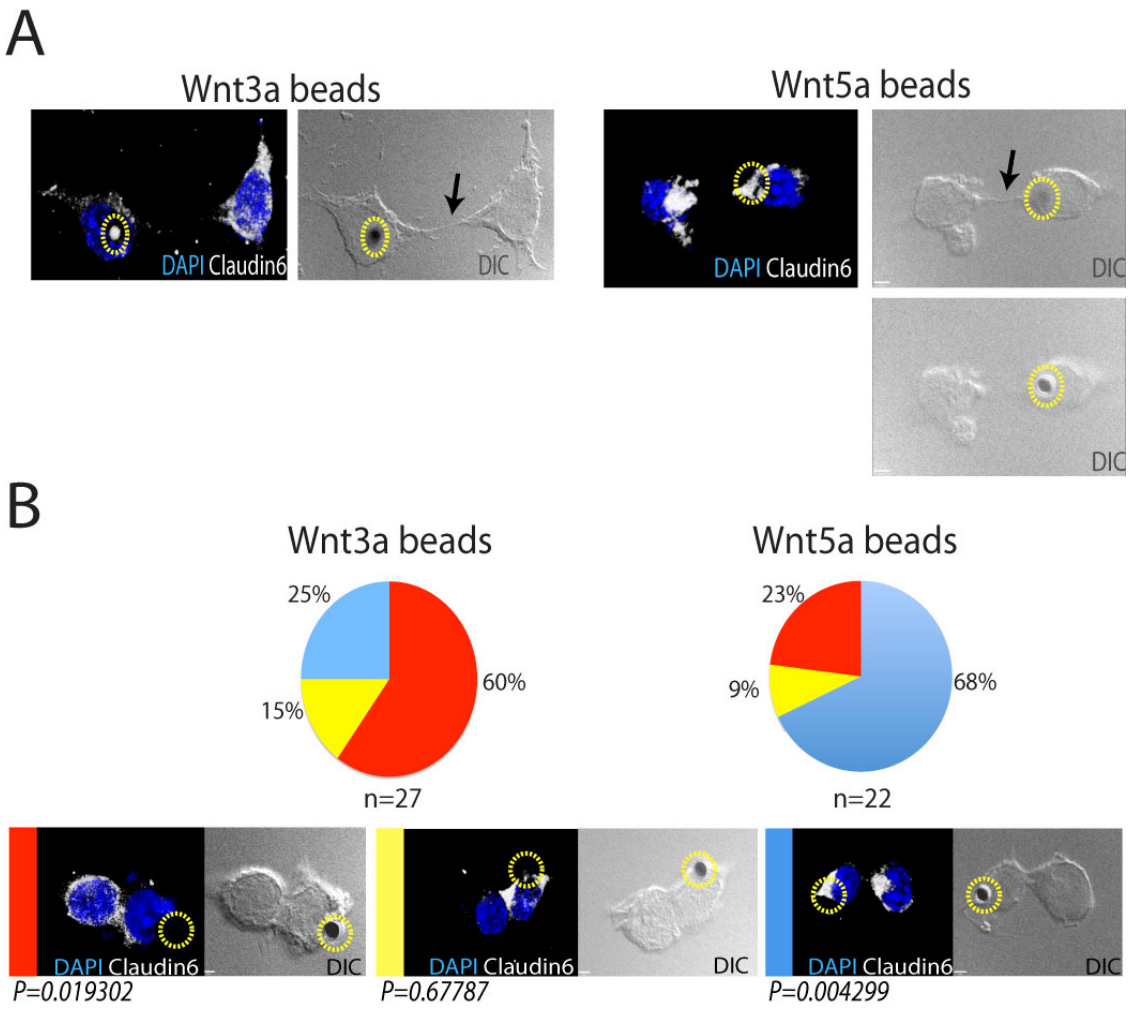

Fig. S12

Wnt-distal cells express markers of Epiblast stem cell fate. **(A)** and **(B)** Single cells of LF2 female ES line were co cultured with Wnt3a or Wnt5a beads. After the division, the cells were fixed and immunostained with antibodies that recognize Claudin6. Based on the relative expression of Claudin6, the dividing cells were sorted into categories for quantification. Red bar: higher Claudin6 levels in the Wnt-proximal cell. Yellow bar: higher levels of Claudin6 in the Wnt distal cell. Blue bar: similar levels of Claudin6 in both cell. The location of the bead that contacted the cell during the division is marked by dashed yellow circle. An arrow indicates the nanotube during cytokinesis (A).

Movie S1

Three-dimensional view of a dividing H2B-Venus ES contacting Wnt3a bead. Images were collected by Bessel beam plane illumination microscopy every 30s.

Movie S2

Three-dimensional view of a dividing H2B-Venus ES contacting Wnt5a bead. Images were collected by Bessel beam plane illumination microscopy every 30s.

Movie S3

A Nanog-Venus ES cell contacting Wnt3a bead. Images were captured every 20 minutes.

Movie S4

A Rex1-GFP ES cell contacting Wnt3a bead. Images were captured every 20 minutes.

Movie S5

A Sox2-GFP ES cell contacting Wnt3a bead. Images were captured every 20 minutes.

Movie S6

A Stella-GFP ES cell contacting Wnt3a bead. Images were captured every 20 minutes.

Movie S7

A Nanog-Venus ES cell contacting Wnt5a bead. Images were captured every 20 minutes.

Movie S8

A Rex1-GFP ES cell contacting Wnt5a bead. Images were captured every 20 minutes.

Movie S9

A Sox2-GFP ES cell contacting Wnt5a bead. Images were captured every 20 minutes.

Movie S10

A Stella-GFP ES cell contacting Wnt5a bead. Images were captured every 20 minutes.

References and Notes

1. R. A. Neumüller, J. A. Knoblich, Dividing cellular asymmetry: Asymmetric cell division and its implications for stem cells and cancer. *Genes Dev.* **23**, 2675 (2009). doi:10.1101/gad.1850809 Medline

2. A. D. Werts, B. Goldstein, How signaling between cells can orient a mitotic spindle. *Semin. Cell Dev. Biol.* **22**, 842 (2011). doi:10.1016/j.semcdb.2011.07.011 Medline

3. T. Walston *et al*., Multiple Wnt signaling pathways converge to orient the mitotic spindle in early C. elegans embryos. *Dev. Cell* **7**, 831 (2004). doi:10.1016/j.devcel.2004.10.008 Medline

4. B. Goldstein, H. Takeshita, K. Mizumoto, H. Sawa, Wnt signals can function as positional cues in establishing cell polarity. *Dev. Cell* **10**, 391 (2006). doi:10.1016/j.devcel.2005.12.016 Medline

5. K. Sugioka, K. Mizumoto, H. Sawa, Wnt regulates spindle asymmetry to generate asymmetric nuclear β-catenin in C. elegans. *Cell* **146**, 942 (2011). doi:10.1016/j.cell.2011.07.043 Medline

6. D. ten Berge *et al*., Embryonic stem cells require Wnt proteins to prevent differentiation to epiblast stem cells. *Nat. Cell Biol.* **13**, 1070 (2011). doi:10.1038/ncb2314 Medline

7. N. Sato, L. Meijer, L. Skaltsounis, P. Greengard, A. H. Brivanlou, Maintenance of pluripotency in human and mouse embryonic stem cells through activation of Wnt signaling by a pharmacological GSK-3-specific inhibitor. *Nat. Med.* **10**, 55 (2004). doi:10.1038/nm979 Medline

8. Q.-L. Ying *et al*., The ground state of embryonic stem cell self-renewal. *Nature* **453**, 519 (2008). doi:10.1038/nature06968 Medline

9. A. Surani, J. Tischler, Stem cells: A sporadic super state. *Nature* **487**, 43 (2012). doi:10.1038/487043a Medline

10. A. J. Mikels, R. Nusse, Purified Wnt5a protein activates or inhibits beta-catenin-TCF signaling depending on receptor context. *PLoS Biol.* **4**, e115 (2006). doi:10.1371/journal.pbio.0040115 Medline

11. S. Bahmanyar *et al*., beta-Catenin is a Nek2 substrate involved in centrosome separation. *Genes Dev.* **22**, 91 (2008). doi:10.1101/gad.1596308 Medline

12. Y. M. Yamashita, D. L. Jones, M. T. Fuller, Orientation of asymmetric stem cell division by the APC tumor suppressor and centrosome. *Science* **301**, 1547 (2003). doi:10.1126/science.1087795 Medline

13. M. M. Mogensen, A. Malik, M. Piel, V. Bouckson-Castaing, M. Bornens, Microtubule minus-end anchorage at centrosomal and non-centrosomal sites: The role of ninein. *J. Cell Sci.* **113**, 3013 (2000). Medline

14. X. Wang *et al*., Asymmetric centrosome inheritance maintains neural progenitors in the neocortex. *Nature* **461**, 947 (2009). doi:10.1038/nature08435 Medline

15. M. Bornens, The centrosome in cells and organisms. *Science* **335**, 422 (2012). doi:10.1126/science.1209037 Medline

16. Y. M. Yamashita, M. T. Fuller, Asymmetric centrosome behavior and the mechanisms of stem cell division. *J. Cell Biol.* **180**, 261 (2008). doi:10.1083/jcb.200707083 Medline

17. T. A. Planchon *et al*., Rapid three-dimensional isotropic imaging of living cells using Bessel beam plane illumination. *Nat. Methods* **8**, 417 (2011). doi:10.1038/nmeth.1586 Medline

18. B. Payer *et al*., Generation of stella-GFP transgenic mice: A novel tool to study germ cell development. *Genesis* **44**, 75 (2006). doi:10.1002/gene.20187 Medline

19. Y. Toyooka, D. Shimosato, K. Murakami, K. Takahashi, H. Niwa, Identification and characterization of subpopulations in undifferentiated ES cell culture. *Development* **135**, 909 (2008). doi:10.1242/dev.017400 Medline

20. K. Hayashi, S. M. Lopes, F. Tang, M. A. Surani, Dynamic equilibrium and heterogeneity of mouse pluripotent stem cells with distinct functional and epigenetic states. *Cell Stem Cell* **3**, 391 (2008). doi:10.1016/j.stem.2008.07.027 Medline

21. K. Arnold *et al*., Sox2(+) adult stem and progenitor cells are important for tissue regeneration and survival of mice. *Cell Stem Cell* **9**, 317 (2011). doi:10.1016/j.stem.2011.09.001 Medline

22. A. M. Singh, T. Hamazaki, K. E. Hankowski, N. Terada, A heterogeneous expression pattern for Nanog in embryonic stem cells. *Stem Cells* **25**, 2534 (2007). doi:10.1634/stemcells.2007-0126 Medline

23. I. Chambers *et al*., Nanog safeguards pluripotency and mediates germline development. *Nature* **450**, 1230 (2007). doi:10.1038/nature06403 Medline

24. K. A. Kim *et al*., Mitogenic influence of human R-spondin1 on the intestinal epithelium. *Science* **309**, 1256 (2005). doi:10.1126/science.1112521 Medline

25. P. J. Tesar *et al*., New cell lines from mouse epiblast share defining features with human embryonic stem cells. *Nature* **448**, 196 (2007). doi:10.1038/nature05972 Medline

26. G. Guo *et al*., Klf4 reverts developmentally programmed restriction of ground state pluripotency. *Development* **136**, 1063 (2009). doi:10.1242/dev.030957 Medline

27. K. Plath *et al*., Role of histone H3 lysine 27 methylation in X inactivation. *Science* **300**, 131 (2003). doi:10.1126/science.1084274 Medline

28. M. A. Hilliard, C. I. Bargmann, Wnt signals and frizzled activity orient anterior-posterior axon outgrowth in C. elegans. *Dev. Cell* **10**, 379 (2006). doi:10.1016/j.devcel.2006.01.013 Medline

29. C. Korkut *et al*., Trans-synaptic transmission of vesicular Wnt signals through Evi/Wntless. *Cell* **139**, 393 (2009). doi:10.1016/j.cell.2009.07.051 Medline

30. K. Willert *et al*., Wnt proteins are lipid-modified and can act as stem cell growth factors. *Nature* **423**, 448 (2003). doi:10.1038/nature01611 Medline

31. B. Payer *et al. Genesis (New York, NY: 2000)* **44**, 75 (2006).

32. H. M. Eilken, S. Nishikawa, T. Schroeder, Continuous single-cell imaging of blood generation from haemogenic endothelium. *Nature* **457**, 896 (2009). doi:10.1038/nature07760 Medline

33. Z. Ma, T. Swigut, A. Valouev, A. Rada-Iglesias, J. Wysocka, Sequence-specific regulator Prdm14 safeguards mouse ESCs from entering extraembryonic endoderm fates. *Nat. Struct. Mol. Biol.* **18**, 120 (2011). doi:10.1038/nsmb.2000 Medline